

Virtual Colon Flattening Based on Colonic Outer Surface

Lin Lu, Kemin Chen, and Jun Zhao*, *Member, IEEE*

Abstract—Virtual colon flattening (VF) is a non-invasive procedure to inspect the colonic inner surface for detecting colorectal polyps. Unfortunately, the performance of VF is impeded by deformation distortions of colonic inner surface. Conventionally, the colonic inner surface itself is used to correct deformation distortions. In this paper, we propose a colonic outer surface based VF method to correct distortions instead of colonic inner surface. The proposed method was validated with 60 cases and 200 annotated polyps. Visual inspections were carried out by three operators independently and were compared with three existing VF methods which are based on colonic inner surface. The correct detection rate of the proposed method and the three existing methods were 88.0%, 76.5%, 80.0% and 81.5% respectively. False positives per case were 0.16, 0.32, 0.21, and 0.26 respectively. The proposed method has higher correct detection rate and less false positives than the other three VF methods, demonstrating the usefulness of colonic outer surface as a correction tool for VF results.

I. INTRODUCTION

The technique of virtual colon flattening (VF) is an alternative way to the virtual colonoscopy for detecting colorectal polyps [1]. The VF technique can provide a global field of view of the entire three-dimensional (3D) colonic inner surface for operators by virtually flattening the colonic inner surface onto a two-dimensional (2D) image. Many methods have been proposed to implement the VF technique in the last decade [1-3]. Unfortunately, the performances of the previous VF methods are often hindered by distortions of colonic inner surface when deformed from a 3D structure to a 2D image. Investigations on colonic distortions indicated that colonic distortions are related to the degree of colonic curvatures and the size of colonic calibers [4]. In the previous methods, the colonic inner surface itself is usually used as the basis for the distortion correction. However, the existence of various colonic haustral folds makes the surface of the colonic inner surface very unsmooth and thus lead to unsatisfied distortion correction.

In this paper, we develop a colonic outer surface based VF method for distortion correction. The advantage of using colonic outer surface rather than colonic inner surface to correct distortion is that, colonic outer surface is immune to the existence of colonic haustral folds. The proposed method

includes two algorithms: 1) the colonic outer surface extraction (OSE) algorithm that is capable of extracting colonic outer surface which is suitable for the VF technique and 2) the distortion correction algorithm (DCA) based on colonic outer surface. The OSE algorithm used level set method [5] to generate candidate colonic outer surfaces first and then eliminate undesired connections between distant surface regions with the help of a geodesic distance map [6]. The DCA algorithm presents the means of how to use the extracted colonic outer surface to correct the flattened colonic inner surface.

II. METHOD

At the beginning of this section, three concepts are defined: colonic inner surface, colonic outer surface and colonic wall. Anatomically, the colonic inner surface is the lumen-mucosa boundary, while the colonic outer surface is the tissue-serosa boundary. The colonic wall is the layer between colonic inner surface and colonic outer surface. In this paper, the colonic inner surface is the outer surface of the colonic lumen and the colonic outer surface is the outer surface of the colonic wall (See Figure 1).

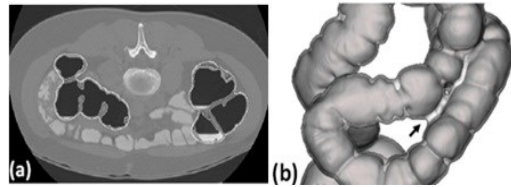


Figure 1. (a) is a 2D CT slice. White lines in (a) plot out the colonic outer surface. Gray lines in (a) plot out the colonic inner surface. The colonic wall is located between the colonic inner surface and colonic outer surface. (b) is a 3D presentation.

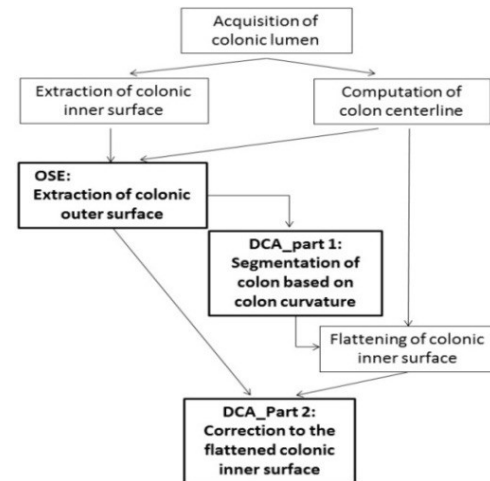


Figure 2. The framework of VF technique based on the proposed method. Bold modules represent the main contributions of the proposed method.

*Asterisk indicates corresponding author.

Lin Lu is with the School of Biomedical Engineering, Shanghai Jiao Tong University, 800 Dong Chuan Road, Shanghai 200240, China (linlu@sjtu.edu.cn)

Kemin Chen is with the Department of Radiology, Ruijin Hospital, 179 Second Ruijin Road, Shanghai 342500, China (keminchenrj@yahoo.com.cn)

Jun Zhao is with the School of Biomedical Engineering, Shanghai Jiao Tong University, 800 Dong Chuan Road, Shanghai 200240, China (junzhao@sjtu.edu.cn)

The framework of VF technique based on our proposed method is presented in Figure 2. As shown in Figure 2, the OSE algorithm used the colonic inner surface and colon centerline to generate colonic outer surface. DCA algorithm is divided into two parts. The first part is used to preprocess the colonic inner surface and the second part is used to correct the flattened colonic inner surface.

A. Colonic outer surface extraction algorithm

In this section, the OSE algorithm is developed to extract a precise, complete and single-connectedness colonic outer surface by combining the advantages of level set method [5], geodesic distance transform [6] and ball filter technique [7]. The basic idea of the OSE algorithm is that, although partial colonic wall might fuse together after the level set computation, the colonic lumen should be still single-connected without any distant connections. The OSE algorithm can be divided into three steps.

First, we used the procedure presented in Van Uiter's work [8] to generate a candidate colonic outer surface based on the 3D geodesic active contour level set method. Second, the geodesic distance transformation is adapted to create a geodesic distance map for the colonic lumen. The geodesic distance map is able to indicate the shortest distance between two arbitrary voxels inside the colonic lumen. Third, detect and remove fused areas of the colonic wall with the use of ball filter technique. The ball filter is constructed as follows.

Let voxel set \mathbf{O} represents all the voxels inside the colon outer surface, voxel set \mathbf{I} represent all the voxels of the colonic lumen and voxel set \mathbf{B} represents all the voxels inside the ball filter with radii T_r and centroid C . The output of the ball filter can be calculated as following:

$$f_b(q) = \text{Max}(g(q)) - \text{Min}(g(q)), q \in \mathbf{B}. \quad (1)$$

$$\mathbf{B} = \{q \mid \|q - C\| < T_r, q \in \mathbf{I}, C \in (\mathbf{O} - \mathbf{I})\}. \quad (2)$$

Here $g(q)$ returns the value of the geodesic distance at the position of voxel q . Voxels with filter outputs larger than a predetermined threshold T_d would be removed as undesired voxels locating at the fused regions of colonic wall. The radii T_r is set to $2 * 6 / \text{Rel}_x$ (Rel_x is the sagittal resolution of CT scan) under the hypothesis that colonic wall should not exceed 6 mm . The threshold T_d is set to $0.05 * g_{\text{max}}$ (g_{max} is the geodesic distance from the rectum to the ceceum) under the hypothesis that colonic folds should not exceed five percentage of the whole length of colon centerline.

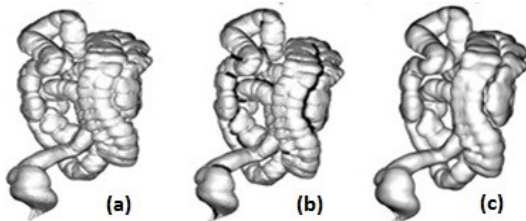


Figure 3. (a) is the candidate colonic outer surface extracted by level set method. (b) indicates the fused areas of colonic wall with black color. (c) shows the final colonic outer surface.

Finally, a complete and single-connected colonic outer surface can be easily extracted from the processed colonic wall. An example for a real case is presented in Figure 3.

B. Distortion correction algorithm

a. Segmentation of colon based on colonic curvature

Colonic curvature might cause extreme distortions to colonic inner surface. Intuitively, we could separate all the curved and straight regions before flattening colonic inner surface, so that each region could be processed independently. In this paper, a novel "velocity" property of the scalar complementary geodesic distance map (CGDM) [6] is developed to determine the boundaries between curve regions and straight regions. Scalar CGDM is a kind of double-seeded geodesic distance transformation.

Given a voxel p and two starting seeds, CGDM can be computed by equation (3):

$$cg(p) = g_1(p) - g_2(p). \quad (3)$$

Here, $g_1(p)$ returns the geodesic distance from the voxel p to the first seed and $g_2(p)$ returns the geodesic distance from voxel p to the second seed. In the DCA algorithm, the rectum endpoint and the cecum endpoint are used as the two starting seeds respectively [9]. Then, by using a distance interval R , CGDM could be normalized to the scalar CGDM, which is composed of a series of equidistant sheets (See Figure 6. a).

The proposed velocity property is used to quantify the degree of colonic curvature. The velocity v of an equidistant sheet can be computed by equation:

$$v = \frac{\sum_{i=0}^t \nabla cg(p_i)}{t}. \quad (4)$$

Here $\nabla cg(p)$ calculates the gradient of scalar CGDM at the voxel p . The symbol t represents the total number of voxels inside the equidistant sheet.

To determine curve regions, three post-processing steps are necessary. First, extract all the local minimums from the curve of velocity. Second, remove local minimums of values larger than threshold T_v . Third, label valleys where those remaining local minimums locate as the curve regions. The threshold T_v in our method is empirically set as numerical value 5.0, which is sufficient to exclude the regions of slight curvature.

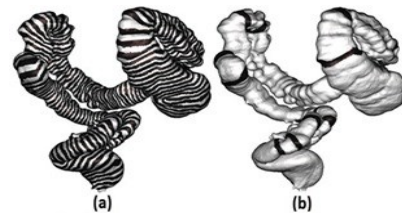


Figure 4. Streaks on the colonic surface in (a) show a series of equidistant sheets in scalar CGDM. Black stripes in (b) indicate the boundaries between curve regions and straight regions.

b. Correction to the flattened colonic inner surface

The correction procedure consists of two steps. First, we acquire the original sampling endpoints by using the electronic field sampling method [1], which uses a charge centerline to generate electronic lines as sampling rays to parameterize the colonic inner surface. Each point on the colonic centerline constructs a sampling plane, as shown in Figure 5(a). The original endpoints are defined by those voxels located at the position where the original sampling rays hit the colonic outer surface. The trajectory of the original endpoints is used as an approximation to the real colonic outer surface, as shown in Figure 5(b).

Second, we create new endpoints along the trajectory of the original endpoints. The new endpoints, also called as adjusted endpoints, are of equal distance along the trajectory of the original endpoints. The distance between two adjusted endpoints is controlled by a fixed value D . The value D is set according to the resolution of the CT data and acts as a modulator to the VF sampling rate. In our proposed method, D is set to $1.0/Rel_x$. Lines defined by the charge points on the colon centerline and their adjusted endpoints are used as new linear sampling rays. A description of the correction to sampling rays on a given sampling plane is presented in Figure 5. Also, the pseudo code presented in Figure 6 is used to illustrate how to compute adjusted endpoints with the use of the original endpoints.

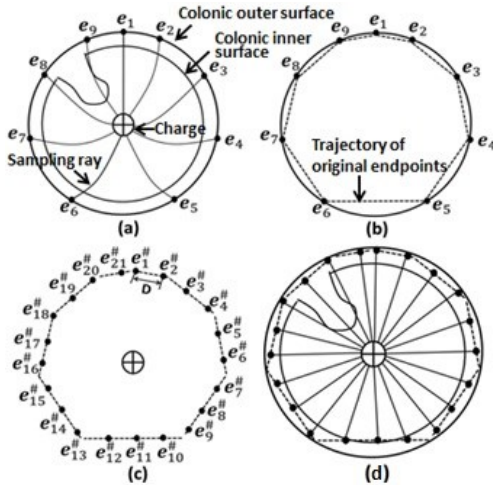


Figure 5. (a) is the sampling plane which is composed of one charge point and a group of sampling rays. Original endpoints are represented as $e_i, i \in \{1, 2, \dots, 7\}$. (b) indicates the trajectory of the original endpoints by dotted lines. (c) shows the adjusted endpoints along the trajectory of the original endpoints. Adjusted endpoints are represented as $e_j^{\#}, j \in \{1, 2, \dots, 21\}$. Distances between two arbitrary neighboring adjusted endpoints along the trajectory are equal to the fixed value D . (f) presents the final result of the new linear sampling rays.

```

 $e_i, i \in \{1, 2, \dots, m\}$ : original endpoints with total number of  $m$ ;
 $e_j^{\#}, j \in \{1, 2, \dots, n\}$ : adjusted endpoints with total number of  $n$ ;
 $D$ : distance between two adjusted endpoints along the trajectory of original endpoints;
 $unit(\mathbf{d})$ : returns the unit vector.
Proc Correction_to_sampling_rays(
    in: original endpoints,
    out: adjusted endpoints)
{
 $\mathbf{d}_i = \begin{cases} unit(\mathbf{e}_{i+1} - \mathbf{e}_i), i = 1, 2, \dots, m-1; \\ unit(\mathbf{e}_1 - \mathbf{e}_i), i = m \end{cases}$ 
 $n = \text{int}(\frac{\sum_{i=0}^m \|\mathbf{e}_i - \mathbf{e}_{i-1}\|}{D}) + 1;$ 
double new_dis = D;
double ori_dis =  $\|\mathbf{e}_2 - \mathbf{e}_1\|$ ;
int ori_index = 2;
int new_index = 2;
 $\mathbf{e}_1^{\#} = \mathbf{e}_1$ ;
while(new_index  $\leq$  n)
{
if(ori_dis > new_dis)
{
 $\mathbf{e}_{new\_index}^{\#} = \mathbf{e}_{ori\_index} - (\text{ori\_dis} - \text{new\_dis}) * \mathbf{d}_{ori\_index-1};$ 
new_dis = new_dis + D;
new_index = new_index + 1;
}
else
{
ori_dis = ori_dis +  $\|\mathbf{e}_{ori\_index} - \mathbf{e}_{ori\_index-1}\|$ ;
ori_index = ori_index + 1;
}
}
}

```

Figure 6. A pseudo code illustrating the calculation of adjusted endpoints.

III. EVALUATION METHOD AND RESULTS

A. Materials

We used 60 CT cases to test the performance of the proposed method mentioned above. The CT cases were all downloaded from the National Cancer Institute's Image Archive Resources (<https://imaging.nci.nih.gov/ncia>). Each CT case contained at least one true polyp with a diameter larger than 5 mm. There were 77 true polyps (16 pedunculated polyps, 54 sessile polyps and 7 flat polyps) locating among the 60 testing cases. Besides, we randomly implanted 123 pseudo polyps into the testing cases. Pseudo polyps were created by using a ball of size 6 ~ 15 mm to erode the colonic inner surface. Totally, there were 200 annotated polyps used for the testing

B. Experiments and Results

All of the testing cases would undergo the same segmentation procedures. Firstly, automatic segmentation method [8] was applied to extract colonic inner surface. Then, operators would manually refine the computer-generated colonic inner surfaces with the help of 2D colonography, so as to remove false positive polyps that might be caused by incorrect colon segmentation as much as possible.

The proposed method was compared with three existing methods, which were based on ray tracing algorithm (RAT), conformal mapping method (CMM) and animated skeleton technique (AST), respectively. The three existing methods were implemented according to existing literatures [1-3] and coded with Matlab Language [10] and VTK Libraries [11]. Due to the lack of details of implementation, some parameters of the three methods were only set empirically with the help of anatomical knowledge. The time for our method (including the OSE and the DCA as mentioned in Figure 2) to correct colonic

deformation distortion was 13 minutes averagely on a PC platform of Intel 1.73GHz CPU and 4.00 GB RAM.

Three operators were asked to visually inspect the VF results of the four methods on the graphics workstation independently. The three operators are all with at least 50-case experience on the inspection of flattened colons. Two indicators, the correct detection rate and the false positives per case, were used to evaluate the results. The two indicators are defined as follows:

$$\text{Correct detection rate} = \frac{\text{Number of detections}}{\text{Number of annotations}} * 100\% \quad (5)$$

$$\text{False positives per case} = \frac{\text{Number of false positives}}{\text{Number of cases}} \quad (6)$$

The results of correct detection rate and false positives per case are presented in the Table 1 and Table 2 respectively. An example of the flattened colonic inner surface with the use of the proposed method is presented in Figure 7.

TABLE 1 CORRECT DETECTION RATE

Method	Correct detection rate			
	Number of Detections / Number of Annotations			
	Outer surface	Inner surface		
Reader	Our method	RTA method	CMM method	AST method
Reader1	89.5% 179/200	81.0% 162/200	82.5% 165/200	85.0% 170/200
Reader2	88.5% 177/200	75.5% 151/200	80.5% 161/200	81.0% 162/200
Reader3	86% 172/200	73.0% 146/200	77.0% 154/200	78.5% 157/200
Average	88.0%	76.5%	80.0%	81.5%

TABLE 2 False positive per case

Method	False positive per case			
	Number of False Positives / Number of Cases			
	Outer surface	Inner surface		
Reader	Our method	RTA method	CMM method	AST method
Reader1	0.13 8/60	0.25 16/60	0.15 9/60	0.21 13/60
Reader2	0.18 11/60	0.37 22/60	0.23 14/60	0.3 18/60
Reader3	0.17 10/60	0.3 19/60	0.25 15/60	0.25 16/60
Average	0.16	0.32	0.21	0.26

IV. CONCLUSION

In this paper, we have presented a VF method that uses the colonic outer surface as the basis to correct distortions caused by nonlinear flattening. In contrast to using the colonic inner surface, there were two main advantages of using the colonic outer surface. First, the target surface and correction basis were separated, unlike those conventional means of using colonic inner surface to correct colonic inner surface itself. Second, the colonic outer surface was a layer of smooth and consistent surface which shows the global profile of the colonic wall. The colonic outer surface was immune to the influences of colonic haustral folds. As shown in Table 1, the method based on the colonic outer surface could yield the highest correct

detection rate and the least false positives per case when compared to other methods which are based on the colonic inner surface. Besides, among different readers, the results obtained by the method using the colonic outer surface was more consistent than the results obtained by those methods using the colonic inner surface. We believe that colonic outer surface is a useful tool for the distortion correction to VF results.

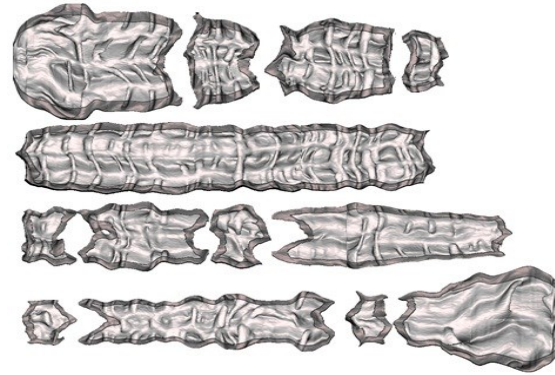


Figure 7. A flattened colonic inner surface with the use of the proposed method. The dark color indicates those overlapping regions.

ACKNOWLEDGMENT

This work is partially supported by the National High Technology Research and Development Program of China (863 Program; 2007AA02Z452), National Basic Research Program of China (973 Program 2010CB834302).

REFERENCES

- [1] G. Wang, E. McFarland, B.P. Brown, and M.W. Vannier, GI tract unraveling with curved cross-sections. *IEEE Trans Med Imaging*, 1998. 17(2): p. 418-322.
- [2] W. Hong, F. Qiu, and A. Kaufman, A pipeline for computer aided polyp detection. *IEEE Trans Vis Comput Graph*, 2006. 12(5): p. 861-868.
- [3] S. Sudarsky, B. Geiger, C. Chef'd'hotel, and L. Guendel, Colon unfolding via skeletal subspace deformation. *Med Image Comput Assist Interv*, 2008. 11(Pt 2): p. 205-212.
- [4] A.C. Silva, C.V. Wellnitz, and A.K. Hara, Three-dimensional virtual dissection at CT colonography: unraveling the colon to search for lesions. *Radiographics*, 2006. 26(6): p. 1669-1686.
- [5] J.A. Sethian, Evolution, implementation, and application of level set and fast marching methods for advancing fronts. *Journal of Computational Physics*, 2001. 169(2): p. 503-555.
- [6] D.G. Kang, D.C. Suh, and J.B. Ra, Three-dimensional blood vessel quantification via centerline deformation. *IEEE Trans Med Imaging*, 2009. 28(3): p. 405-419.
- [7] P.K. Saha, J.K. Udupa, and D. Odhner, Scale-Based Fuzzy Connected Image Segmentation: Theory, Algorithms, and Validation. *Computer Vision and Image Understanding*, 2000. 77: p. 145-174.
- [8] R.L.V. Uitert and R. M. Summers, Automatic correction of level set based subvoxel precise centerlines for virtual colonoscopy using the colon outer wall. *IEEE Trans Med Imaging*, 2007. 26(8): p. 1069-1078.
- [9] L. Lu, D. Zhang, L. Li, and J. Zhao, Fully automated colon segmentation for the computation of complete colon centerline in virtual colonoscopy. *IEEE Trans Biomed Eng*, 2012. 59(4): p. 996-1004.
- [10] <http://www.mathworks.com/>
- [11] <http://www.vtk.org/>